Mansoura University
Faculty of Engineering
Mansoura Engineering Journal

Designing of Single Switching DBD Ozone Generator

Mohamed B. El-Mashede, *Magdy M. Zaky*, *A. A. Saleh* and M. EL-Hanash*

KEYWORDS:
DBD ozone chamber, Ozone generator, Resonance frequency, High voltage high frequency transformer, and Pulse width modulation (PWM)

***Abstract*— This paper presents a practical designing of dielectric barrier discharge DBD ozone generator. The parametric determination of DBD ozone reactor or chamber is of significant importance because the power supply design is based on these parameters. The power supply is divided into two stages: one of them is responsible for generating a variable pulse signal (pulse width modulation PWM). This modulated signal (control signal) will be adjusted to possess the first harmonic of its Fourier series that equals the resonant frequency of ozone chamber. This harmonic is that corresponding to the resonance operating frequency of DBD ozone reactor parameter values. The second stage is concerned with inverting of the DC voltage to AC high voltage. Owing to the control signal hasn't the capability of directly driving the ozone chamber, the control signal will be connected to MOSFET gate. As a result of this connection, the applied DC to the primary side of high voltage high frequency (HVHF) transformer will be converted to puled signal with pulse voltage equal to that of the applied DC voltage value. Our scope in this work is to design and practically verify the microcontroller module of Pulse width modulation (PWM) generator and MOSFET with HVHF transformer inverting circuit. In addition, practical electrical waveforms of DBD ozone generator modules will be demonstrated. MicroC compiler, Proteus and Cadance_ORCAD_ Allegro PSpice software will be used in this work.**

I. INTRODUCTION

RECENTLY, ozone (O3) is known as a strong oxidizer agents. It is increasingly being used in home and industrial applications, including disinfection, deodorization, and food pretreatment, washing system, ground water treatment, bleaching from paper pulp, swimming pool water treatment [1-3]. Newly, DBD is the most widely studied for ozone generation. DBD is known to generate non-thermal equilibrium plasma even under atmospheric pressure. DBD is suitable for ozone production [4-7]. However, some of ozone generator configurations generate inhomogeneous heating of the dielectric barrier resulting in low ozone production efficiency. Experimental studies regarding the construction of the ozone generator such as electrode arrangements[6-10], dielectric material [11], chamber geometry[12-17], power source construction [18-20], gas type (dry air or oxygen) [11], feed gas flow rate and operation pressure [21] have been extensively studied to obtain an optimal level discharge conditions for high-throughput ozone production.

Ozone is created when diatomic oxygen (O2) is exposed to an electrical field or ultraviolet light. Exposure to these high levels of energy causes a portion of the diatomic oxygen molecules to split into individual oxygen atoms. These free oxygen atoms combine with diatomic oxygen molecules to form ozone. DBD ozone chamber is a device which consists of air or oxygen gap between two conductors. One of the two conductors will be coated with a dielectric material. A high

Received: (09 September, 2021) - Revised: (14 October, 2021) - Accepted: (10 November, 2021)

Mohamed B. El-Mashede, Professor of Electrical Engineering Dept., Faculty of Engineering, Al Azhar University, Nasr City, Cairo, Egypt, (e-mail: mohamedelmashade@gmail.com).

Magdy M. Zaky, Assistant Professor at Egypt Second Research Reactor, EAEA, Egypt, (e-mail: zaky_magdy@yahoo.com).

A. A. Saleh, Assistant Professor at Dept. of Nuclear Safety Research and Radiological Emergencies – NCRRT Center – EAEA, (alaa91071@gmail.com).

***Corresponding Author:** M. EL-Hanash, PhD Candidate at Dept. of Nuclear Safety Research and Radiological Emergencies – NCRRT Center – EAEA, (e-mail: hanash_2020@yahoo.com)*

voltage is applied to the electrodes to overcome the gap insulation [22-24]. As a result, micro discharges will be generated causing ultraviolet radiations that transform the oxygen molecules into ozone. Geometry construction of DBD ozone chamber has many shapes. In this work a co-core cylindrical type will be used as shown in Fig.1. In this figure, the internal cylinder is treated as copper positive electrode that is coated with teflon as a dielectric material. The outer cylinder is made from stainless steel as negative electrode. Air or oxygen will be forced to flow in between the dielectric layer and negative cylindrical electrode. The two holder sides of this construction are made of teflon. Ozone will be comes from the nozzle of the out holder.

Fig. 2 shows the electrical equivalent circuit of DBD ozone chamber. This circuit is composed of two capacitors and discharge resistance R. The discharge resistance is connected in parallel to gap capacitance Cg as gap equivalent circuit whilst dielectric layer (teflon) will be replaced by capacitor Cd. These parameters of DBD ozone chamber can be determined using one of these two techniques; Lissajous plot or differential evolution (DE) method. Lissajous plot achieves good results in frequency range (15-20 KHz) [25-27]. This is attributed to the plotting shape which will be distorted outside this frequency range. As a result of this distortion, uncertainty sources will be increased in the parameters determination. Differential evolution (DE) technique, on the other hand, depends on the resonance frequency. This means that as the resonance frequency increases, accuracy of parameter values will be enhanced [25-27]. In this work, DBD ozone chamber parameters will be extracted from measuring of high voltage and current waveforms which applied to DBD ozone chamber.

Fig. 3 illustrates DBD ozone generator architecture [28-32]. In this figure, the control circuit block is responsible for generating the pulse width modulation (PWM) signal. The modulation may be in frequency, duty cycle, or both of them. The inverter block receives the modulated signal and directly drives its internal single switch inverter. As a result of this action, the DC voltage which applied to the primary side of the HVHF transformer block will be inverted to AC voltage. The output of this transformer will be applied to the ozone chamber [33]. It is of important to note that the two blocks associated with input voltage and rectifier circuit are designed to supply the ozone generator with the DC voltage.

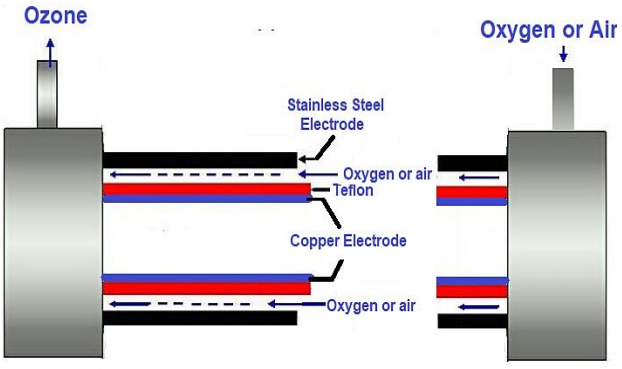

Fig. 1. DBD Ozone chamber

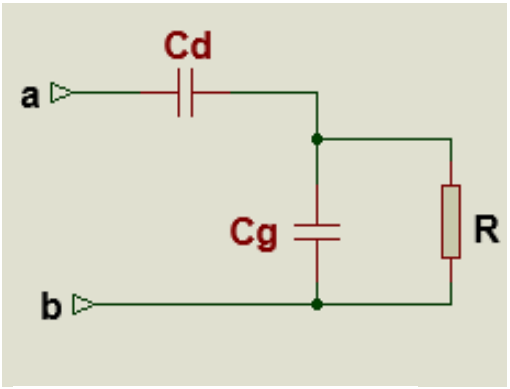

Fig. 2. DBD Ozone chamber equivalent circuit

In order to supply this chamber with high voltage resonance frequency, a controlled signal will be required to control the driving block. Generating a control signal may be achieved either by analog circuit or digital programming control unit. In this work, PIC16F877A microcontroller will be used and programmed with MicroC programming tool. Designing printed circuit board (PCB) and simulation of PWM module are executed using Proteus software whilst simulation of analog waveforms will be proceeded using Cadance_ORCAD_ Allegro PSpice software. A novel entire equivalent circuit of DBD ozone generator will be simulated and presented in this paper. The entire equivalent circuit requires determination of both of the HVHF transformer and DBD ozone chamber parameters. All these parameters have been extracted and verified practically.

This paper will be organized as follows: section 2 illustrates circuit diagram of PWM module and discusses HVHF and DBD ozone chamber parameter values. Section 3 displays our results along with their discussion, and section 4 outlines our concluded remarks.

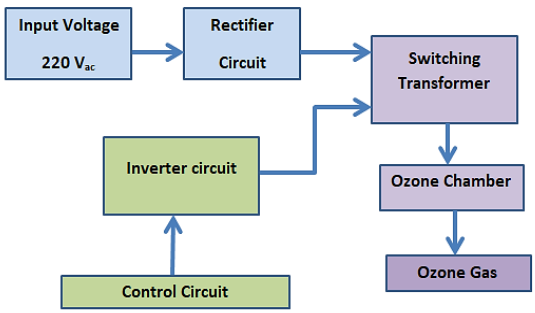

Fig. 3. Ozone generator architecture

II. OZONE GENERATOR CIRCUIT DIAGRAM

Since optimization of ozone generator operating condition plays an important role in its design, a programed PIC microcontroller is used to achieve this purpose. A PWM circuit diagram PIC 16F877A module is illustrated in Fig. 4. This module is designed using Proteus simulation program. It generates frequencies in this range [64Hz - 100 kHz]. The modulation in frequency and duty cycle can be controlled with two techniques: buttons or variable resistances via analog to digital converters (A/D). Because of PIC16F877A

microcontroller has 10 bit A/D converter module, the number of quantization levels are 1024 ones. This means that, to generate the required above mentioned frequency range, the system will has (quantize level / 97 Hz). As a result, the resonance frequency may be unreached. Because of the difficulty of obtaining a resonance frequency through this technique, another mechanism is added (buttons). In order to get the resonance frequency of DBD ozone generator from the final design of this combination, potentiometers of frequency and duty cycle will be rotated smoothly as a first stage. Once, the measured high voltage which is applied to the chamber becomes a sinusoidal waveform in addition to the maximum voltage gain has been obtained, the second stage will start by using the buttons. Increment and decrement buttons will be employed to generate the desired frequency around the gained frequency. Input and output signals of this module are illustrated in Table 1. Fig. 5 illustrates inverting and ozone chamber circuit diagram. The input of this figure is received from the output PWM of Fig. 4. In the underlined plot, the MOSFET is responsible for switching the applied DC voltage on the primary side of the HVHF transformer. The result of this switching is pulsed voltage that will be converted to be of a sinusoidal form according to the ionization resonant frequency, which is coincident with the first harmonic of the pulsed waveform.

TABLE 1
INPUT AND OUTPUT SIGNALS OF PWM MODULE.

Input signals		**Output signal**	
Name (Type)	***Function***	***Name***	***Function***
V_FREQ.(analog)	Changing the frequency	PWM	PWM output
V_DUTY (analog)	Changing the duty cycle		
+ (digital)	Increment the value of the frequency or the duty cycle		
- (digital)	Decrement the value of the frequency or the duty cycle		
Move (digital)	Moving selection between the frequency and the duty cycle		
GO (digital)	Executing and running the selected values of (frequency and duty cycle)		
SW1 (digital)	Selection between analog or digital execution		

Table 2 indicates the parameter values of HVHF transformer and ozone chamber.

Fig. 6 depicts the driving circuit and ozone chamber schematic diagram. In this figure, V1 represents the output PWM signal of PIC16F877A microcontroller which is indicated in Fig.4. Optocoupler will be used as an isolation stage between PWM module and driving of HVHF transformer. HVHF transformer parameters have been extracted practically using open and short circuit tests. These parameters include copper resistance and leakage inductance, the values of which are determined through short circuit test. The magnetizing inductance, core resistance, and stray capacitance are extracted via the open circuit test. The ozone chamber parameters are experimentally evaluated by measuring the waveforms of the applied high voltage at chamber terminals and the ionization current flow through the chamber. Extracting of DBD ozone chamber parameters (Cg & Cd & R) can by evaluated by comparing real and imaginary parts of the total impedance of DBD ozone chamber of Eq.(1) by the corresponding practical measured parts of chamber impedance in Eq. (2). The measured impedance value is calculated by dividing the voltage V_{rms}which applied to the DBD ozone chamber by the current I_{rms} that flows through it.

$$Z_T = Z_g + Z_d = \frac{RX_g^2}{R^2 + X_g^2} - j\,\frac{R^2 X_g}{R^2 + X_g^2} - jX_d \qquad (1)$$

Where, Zg and Zd are gap and dielectric layer impedances, respectively. Xg and Xd are gap and dielectric layer reactances, respectively. Because of the dielectric capacitance Cd is constant and independent of operation conditions like pressure, temperature,…etc., so the value of Cd can be calculated from Eq.(3).

$$Z_T = \frac{V_{rms}}{I_{rms}} \angle\text{-}\alpha = \frac{0.919 * 10^3}{6.25 * 10^{-3}} \angle\text{-}83^o = 17.9 * 10^3 - j\,146.05 * 10^3\ \Omega \qquad (2)$$

$$C_d = \frac{2\pi\epsilon_0 k_e L}{\ln(\frac{b}{a})} \qquad (3)$$

While, b & a are outer and inner radius of teflon dielectric cylinder, respectively. L is the DBD ozone chamber length, whilst, k_e & ϵ_0 are the relative dielectric and the ionization gap permittivities, respectively.

Fig. 7 shows final practical designing of PWM module. Fig 8 illustrates high voltage transformer and ozone chamber parts.

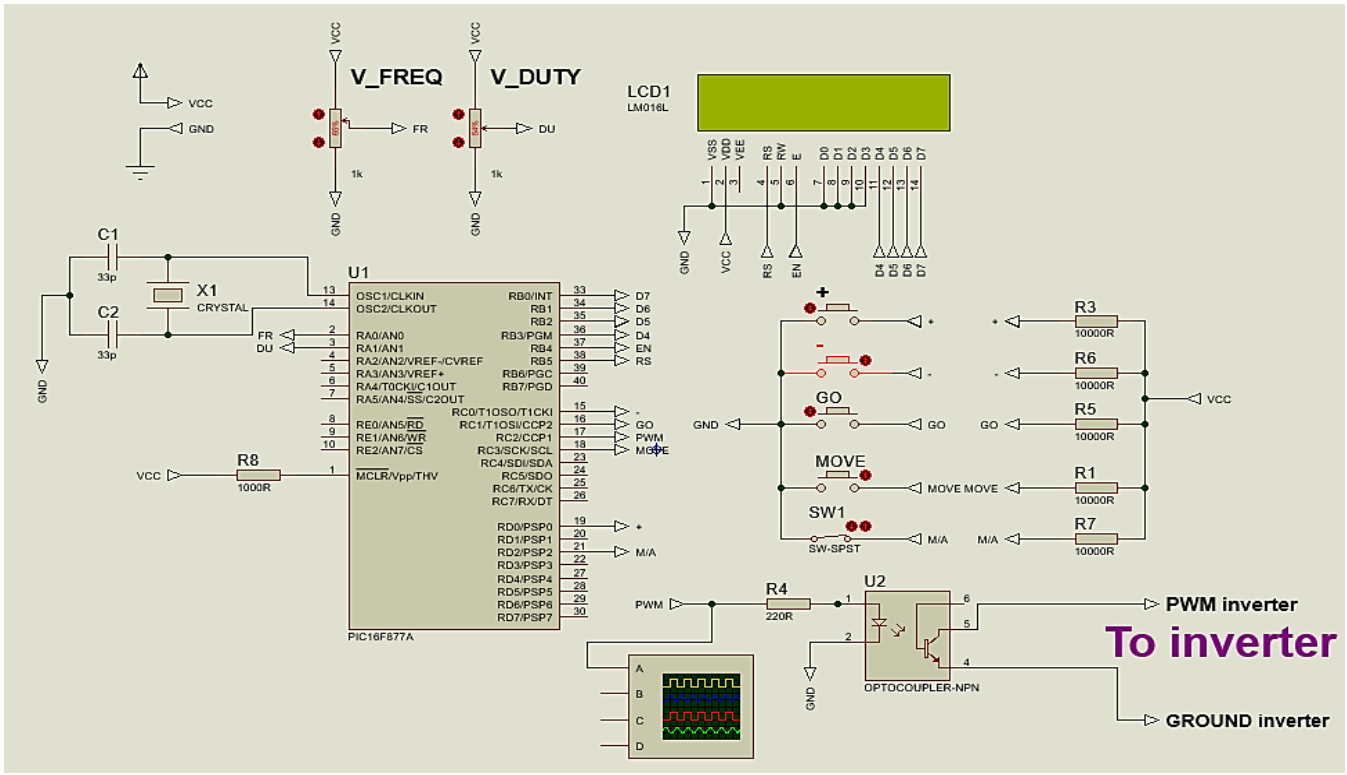

Fig. 4. Circuit diagram of PWM module

TABLE 2
PARAMETERS VALUES OF OZONE CHAMBER AND HVHF TRANSFORMER EQUIVALENT CIRCUITS.

HVHF transformer parameters		**Ozone chamber parameters**	
parameter	***value***	***parameter***	***value***
Leakage inductance L_s	843 μH	*Dielectric capacitance*	1.26 nF
Copper resistance R_s	6.48 Ω	*Discharge resistance R*	950 kΩ
Core resistance R_c	681 Ω	*Gap capacitance Cg*	195 *pF*
Magnetizing inductance L_m	80 μH		
Stray capacitance C_s	89.3 *pF*		

III. ANALYSIS AND RESULTS

Fig 9 presents simulation of the input voltage to the MOSFET gate (green probe) and the voltage applied to the primary side of HVHF transformer (yellow probe). Fig 10 shows the corresponding practical waveforms in which the input voltage to the MOSFET gate is indicated by (Ch2) while, the applied voltage to the primary side of HVHF transformer is demonstrated by (Ch3). As indicated from Figs. (9&10), a good agreement had been observed between practical and simulated results. This similarity means that the equivalent circuit parameter values have been perfectly extracted from the practical point of view. Fig 11 shows simulation of the applied voltage to the primary side of HVHF transformer (yellow probe) and the output applied voltage to the DBD ozone reactor (red probe). Fig 12 illustrates the corresponding practical waveforms in which the input applied voltage to the primary side of HVHF transformer is indicated by (Ch3) and the output applied voltage to the DBD ozone reactor is demonstrated by (Ch1) at resonant frequency of 6124 Hz. Ch1 is measured by using high voltage probe ratio of 1000:1. As shown in Figs. (11&12), the cut off voltage is less than zero volt, which means that there is another reverse voltage source. This voltage can be interpreted as discharging of the charged parasitic capacitances between MOSFET terminals. Fig. 13 shows ozone concentration production (12.05 g/m3) of our case study at air flow rate of (15 L/ minute).

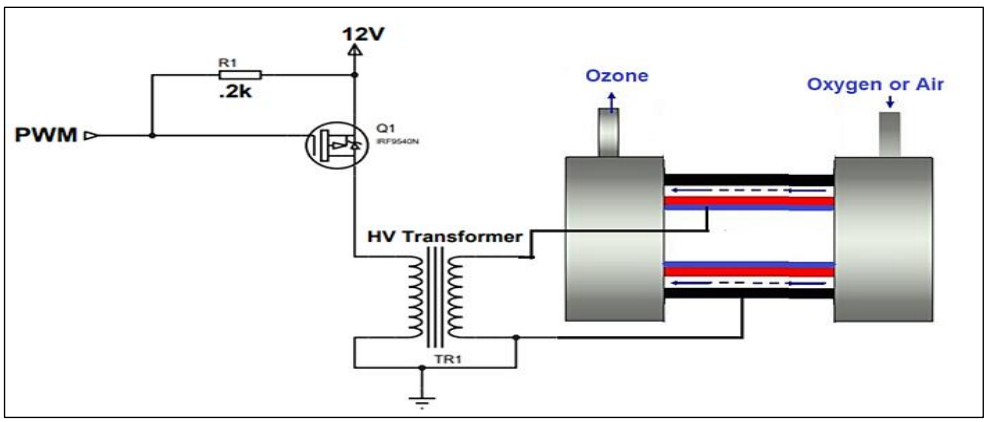

Fig. 5. Inverting circuit and ozone chamber connection.

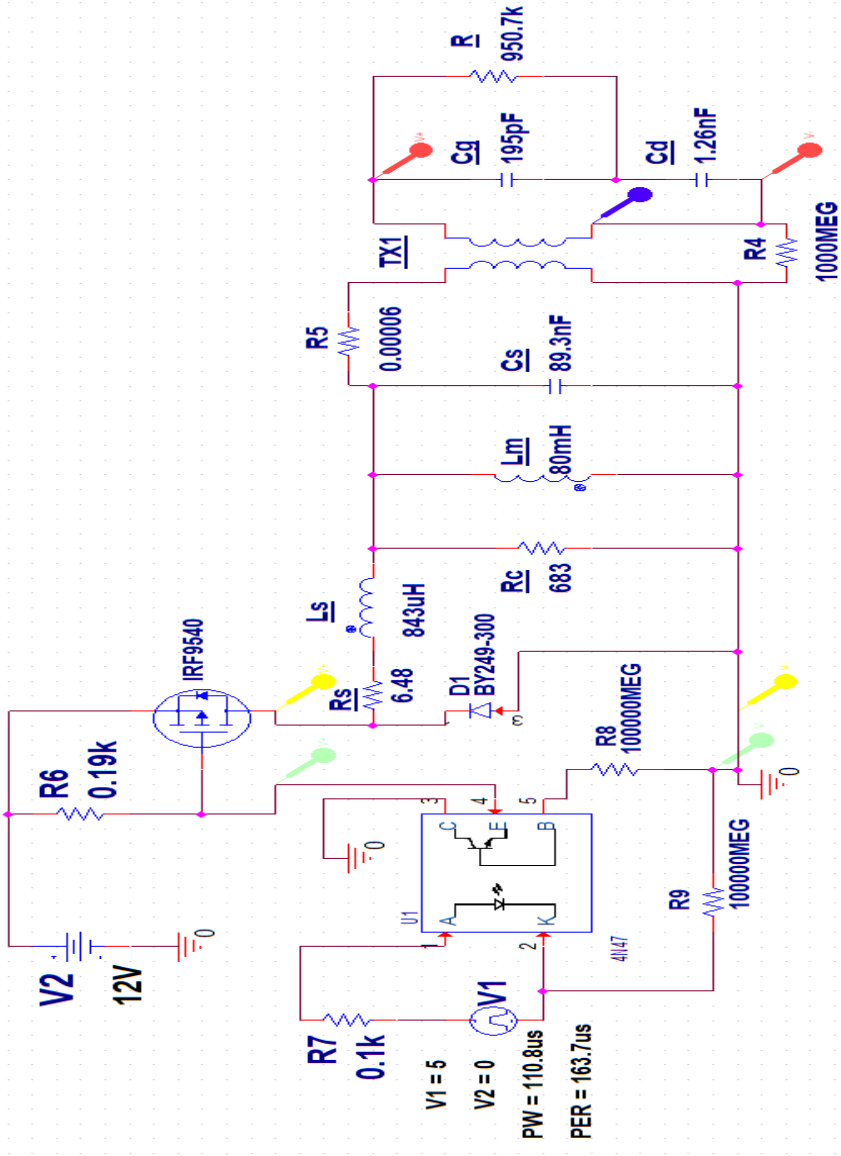

Fig. 6. Ozone generator circuit diagram

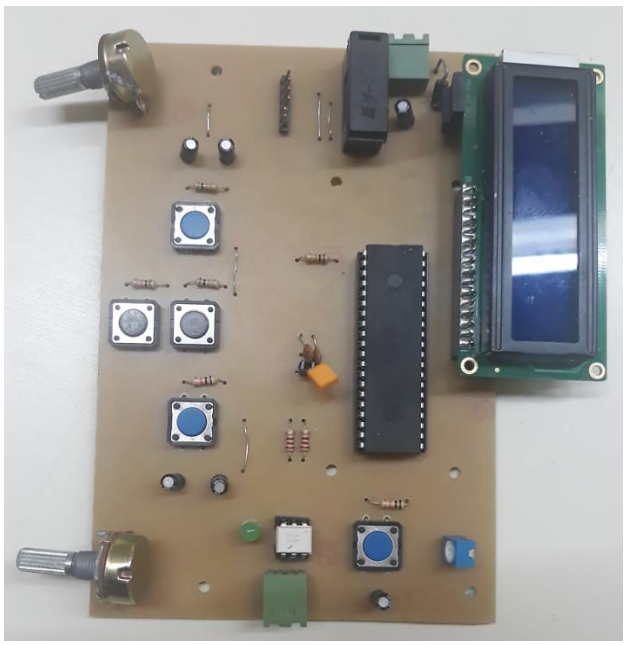

Fig. 7. Practical designing of PWM module

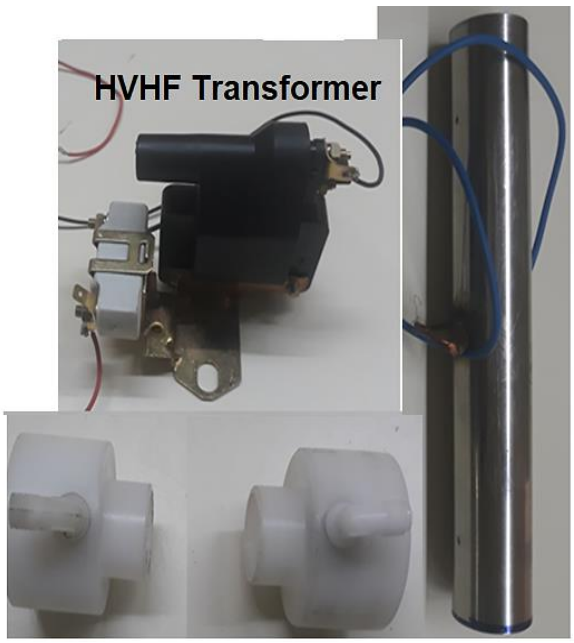

Fig. 8. Ozone chamber components and HVHF transformer

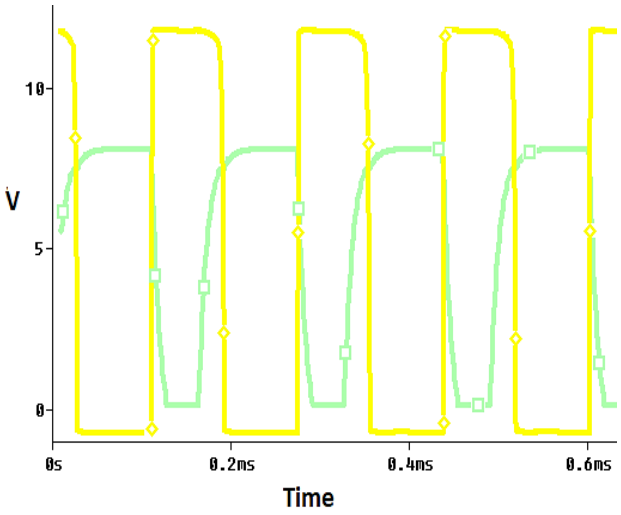

Fig. 9. Input voltage to the MOSFET gate (green probe) and the voltage applied to the primary side of HVHF transformer (yellow probe)

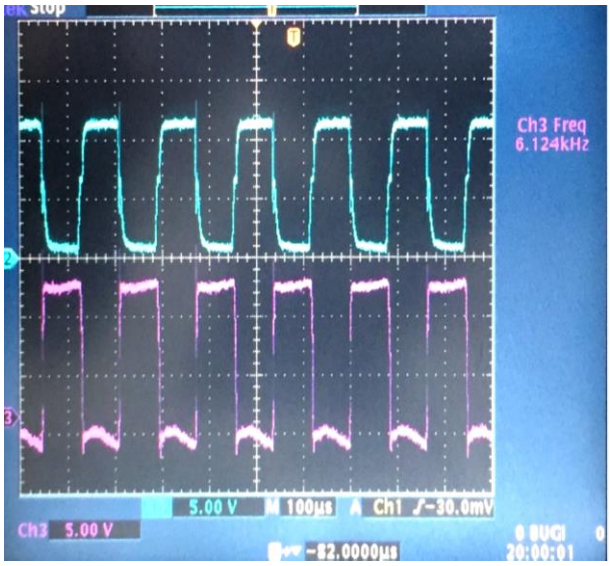

Fig. 10. Practical waveforms of the input voltage to the MOSFET gate (Ch2) and the voltage applied to the primary side of HVHF transformer (Ch3).

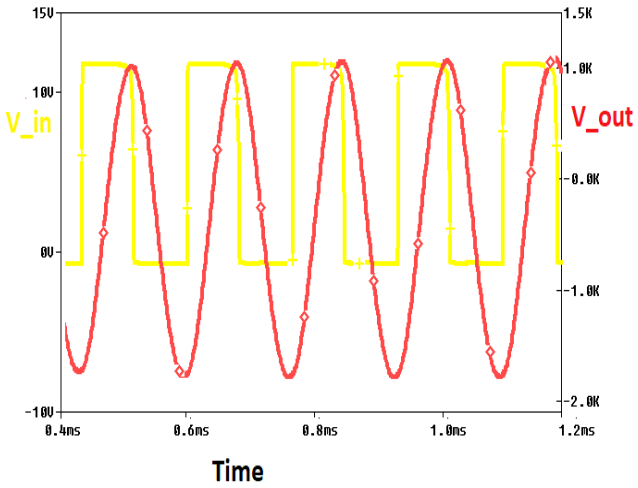

Fig. 11. The input applied voltage to the primary side of HVHF transformer (yellow probe) and the output applied voltage to the DBD ozone reactor (red probe)

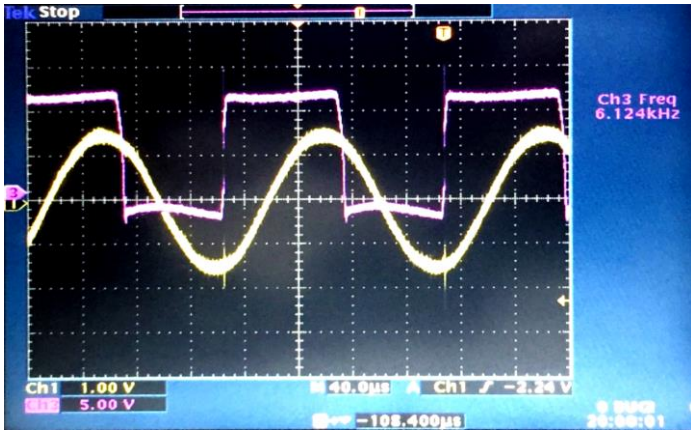

Fig. 12. Practical waveforms of the input applied voltage to the primary side of HVHF transformer (Ch3) and the output applied voltage to the DBD ozone reactor (Ch1).

Fig. 13. Ozone concentration production

IV. CONCLUSION

DBD ozone generator is designed and simulated using Cadance_ORCAD_ Allegro Pspice software. Co-core cylindrical geometry chamber is suggested as DBD ozone reactor. The entire equivalent circuit of HVHF transformer and linear model of DBD ozone reactor are presented and simulated. Practical results and simulated waveforms achieved good agreements. Ozone concentration production rate of our case study is demonstrated and measured using OGP-UV2100 ozone analyzer.

V. AUTHORS CONTRIBUTION

Mohamed B. El_Mashede suggested the paper title and presented the conclusion after his final revision of the research;

Magdy M. Zaky and M. EL_Hanash prepared laboratory tools, analysis the results, and wrote sections (II and III),

A. A. Saleh wrote the introduction.

All Authors Had Approved The Final Version.

FUNDING STATEMENT:

The author did not receive any financial support of the research authorship and publication of this article.

DECLARATION OF CONFLICTING INTERESTS STATEMENT:

The author declared that there are no potential conflicts of interest with respect to the research authorship or publication of this article.

REFERENCES

[1] Rice, R.G., *Ozone in the United States of America--state-of-the-art*. 1999.

[2] Böhme, A., Ozone technology of German industrial enterprises. 1999.

[3] Loeb, B.L., *Ozone: Science & Engineering: Thirty-three years and growing*. Ozone: Science & Engineering, 2011. 33(4): p. 329-342.

[4] Xu, X., *Dielectric barrier discharge—properties and applications. Thin solid films*, 2001. 390(1-2): p. 237-242.

[5] Moreau, M., N. Orange, and M. Feuilloley, *Non-thermal plasma technologies: new tools for bio-decontamination. Biotechnology advances*, 2008. 26(6): p. 610-617.

[6] Fang, Z., et al., *Experimental study on discharge characteristics and ozone generation of dielectric barrier discharge in a cylinder–cylinder reactor and a wire–cylinder reactor*. Journal of Electrostatics, 2008. 66(7-8): p. 421-426.

[7] Takaki, K., et al., *Influence of electrode configuration on ozone synthesis and microdischarge property in dielectric barrier discharge reactor*. Vacuum, 2008. 83(1): p. 128-132.

[8] Jenei, I. and E. Kiss, *Development of the ozone generation by the variation of auxiliary electrodes. Journal of electrostatics*, 2005. 63(6-10): p. 985-991.

[9] Park, S.-L., et al., *Effective ozone generation utilizing a meshed-plate electrode in a dielectric-barrier discharge type ozone generator*. Journal of Electrostatics, 2006. 64(5): p. 275-282.

[10] Takayama, M., et al., *Ozone generation by dielectric barrier discharge for soil sterilization. Thin Solid Films*, 2006. 506: p. 396-399.

[11] Sung, Y.-M. and T. Sakoda, *Optimum conditions for ozone formation in a micro dielectric barrier discharge*. Surface and Coatings Technology, 2005. 197(2-3): p. 148-153.

[12] Murata, T., et al., *Basic parameters of coplanar discharge ozone generator*. Ozone: Science and Engineering, 2004. 26(5): p. 429-442.

[13] Shimosaki, M., et al., *Effect of trigger electrodes configuration of a double discharge ozonizer on ozone generation characteristics*. Vacuum, 2004. 73(3-4): p. 573-577.

[14] Suarasan, I., et al., *A novel type ozonizer for wastewater treatment. Journal of electrostatics*, 2005. 63(6-10): p. 831-836.

[15] Moon, J.-D. and J.-S. Jung, *Effective corona discharge and ozone generation from a wire-plate discharge system with a slit dielectric barrier. Journal of electrostatics*, 2007. 65(10-11): p. 660-666.

[16] Jung, J.-S. and J.-D. Moon, *Corona discharge and ozone generation characteristics of a wire-plate discharge system with a glass-fiber layer*. Journal of electrostatics, 2008. 66(5-6): p. 335-341.

[17] Rainer, G., et al., *Development of atmospheric plasma sprayed dielectric ceramic coatings for high efficiency tubular ozone generators*. Journal of Water Resource and Protection, 2010. 2010.

[18] Kaneda, S., et al., *Application of dielectric material to double-discharge-type ozonizer*. Vacuum, 2004. 73(3-4): p. 567-571.

[19] Alonso, J.M., et al., *Analysis, design, and experimentation of a high-voltage power supply for ozone generation based on current-fed parallel-resonant push-pull inverter*. IEEE transactions on industry applications, 2005. 41(5): p. 1364-1372.

[20] Wang, C., et al., *The effect of air plasma on barrier dielectric surface in dielectric barrier discharge*. Applied Surface Science, 2010. 257(5): p. 1698-1702.

[21] Alsheyab, M.A. and A.H. Muñoz, *Optimisation of ozone production for water and wastewater treatment. Desalination*, 2007. 217(1-3): p. 1-7.

[22] Wen, T.-Y. and J.-L. Su, Corona discharge characteristics of cylindrical electrodes in a two-stage electrostatic precipitator. Heliyon, 2020. 6(2): p. e03334.

[23] Hu, B., et al., Gas pressure measurement using micro-corona-discharging effect in surface acoustic wave resonators. Results in Physics, 2021. 25: p. 104221.

[24] Aziz, K.H.H., et al., Degradation of Perfluoro surfactant in Aqueous Solution using Non-thermal Plasma Generated by Nano-second pulse Corona Discharge Reactor. Arabian Journal of Chemistry, 2021: p. 103366.

[25] Zainal Salam ; Mochammad Facta ; *Muhammad Amjad ; Zolkafle Buntat, "Design and implementation of a low cost, high yield dielectric barrier discharge ozone generator based on the single switch resonant converter*", IET Power Electronics, Vol. 6, Iss. 8, PP. 1583-1591, September 2013.

[26] M. Amjad, Z. Salam, K. Ishaqu, "*A Model Parameter Extraction Method for Dielectric Barrier Discharge Ozone Chamber using Differential Evolution*", Measurement Science Review, Volume 14, No. 2, 2014.

[27] Mohamed B. El_Mashede, et al., Engineering Aspects and Parameter Evaluation of Ozone Generator. WSEAS TRANSACTION on ELECTRONICS, 2021. 12: p, 19-23.

[28] Boonduang, S., et al., *Effect of oxygen pressure and flow rate on electrical characteristic and ozone concentration of a cylinder-cylinder DBD ozone generator.* Procedia Engineering, 2012. **32**: p. 936-942.

[29] Park, S.-L., et al., *Effective ozone generation utilizing a meshed-plate electrode in a dielectric-barrier discharge type ozone generator.* Journal of Electrostatics, 2006. **64**(5): p. 275-282.

[30] Jodpimai, S., S. Boonduang, and P. Limsuwan, *Dielectric barrier discharge ozone generator using aluminum granules electrodes.* Journal of Electrostatics, 2015. **74**: p. 108-114.

[31] Poznyak, T., et al., *Switching robust control for ozone generators using the attractive ellipsoid method.* ISA transactions, 2014. **53**(6): p. 1796-1806.

[32] Krishna, T., et al., *4T analog MOS control-high voltage high frequency (HVHF) plasma switching power supply for water purification in industrial applications.* Electronics, 2018. **7**(10): p. 245.

[33] Choi, C.-y., S. Kwak, and D.-s. Lee. *A study on the resonant inverter for corona generators*. in *2007 7th Internatonal Conference on Power Electronics*. 2007. IEEE.

Title Arabic:

تصميم مولد اوزون تفريغ الحاجز العازل باستخدام المفتاح الفردى

Arabic Abstract:

يقدم هذا البحث تصميمًا عمليًا لمولد أوزون تفريغ الحاجز العازل DBD. بعد تحديد معاملات مفاعل أو غرفة الأوزون، يأتى دور تصميم مصدر الطاقة بناءً على هذه المعاملات. ينقسم مصدر الطاقة إلى مرحلتين: أحدهما مسؤول عن توليد إشارة نبض متغيرة (تعديل عرض وتردد النبضة PWM) والتي سيتم تعديلها للحصول على سلسلة فوريير التوافقية ذات توافق أولي يساوي تردد الرنين وفقًا لمعاملات غرفة الأوزون التى تم تحديدها من قبل .المرحلة الثانية هي تحويل جهد التيار المستمر إلى جهد عالي متناوب باستخدام إشارة النبض المعدلة. تم تصميم وحدة تحكم للتغييرفى عرض النبضة وترددها (PWM) مع دائرة قلب محول الجهد العالي باستخدام ترانزستور من النوع MOSFET والتحقق منها عمليًا. تم عمل محاكاة لدائرة التحكم باسخدام برنامج Proteus وعمل محاكاة للدائرة المكافئة باستخدام برنامج Cadance_ORCAD_ Allegro PSpice كما قمنا بتوضيح أشكال الموجات الكهربائية العملية لوحدات مولد الأوزون. تم برمجة وحدة التحكم باستخدام برنامج التحويل البرمجي MicroC .